Poly(aspartic acid)-based Degradable Assemblies for Highly Efficient Gene Delivery

Jing-Jun Nie,[†,⊥] Xue-Bo Dou,[†,⊥] Hao Hu,[†] Bingran Yu,[†,‡,§] Da-Fu Chen,*[∥] Ren-Xian Wang,[∥] and Fu-Jian Xu*[†,‡,§]

[†]State Key Laboratory of Chemical Resource Engineering, College of Materials Science & Engineering, Beijing University of Chemical Technology, Beijing 100029, China

[‡]Key Laboratory of Carbon Fiber and Functional Polymers (Beijing University of Chemical Technology), Ministry of Education, Beijing 100029, China

[§]Beijing Laboratory of Biomedical Materials, Beijing University of Chemical Technology, Beijing 100029, China

[∥]Laboratory of Bone Tissue Engineering, Beijing Research Institute of Orthopaedics and Traumatology, Beijing JiShuiTan Hospital, Beijing 100035, China

S *Supporting Information*

ABSTRACT: Due to its good properties such as low cytotoxicity, degradability, and biocompatibility, poly(aspartic acid) (PAsp) is a good candidate for the development of new drug delivery systems. In this work, a series of new PAsp-based degradable supramolecular assemblies were prepared for effective gene therapy via the host−guest interactions between the cyclodextrin (CD)-cored PAsp-based polycations and the pendant benzene group-containing PAsp backbones. Such supramolecular assemblies exhibited good degradability, enhanced pDNA condensation ability, and low cytotoxicity. More importantly, the gene transfection efficiencies of supramolecular assemblies were much higher than those of CD-cored PAsp-based counterparts at various N/P ratios. In addition, the effective antitumor ability of assemblies was demonstrated with a suicide gene therapy system. The present study would provide a new means to produce degradable supramolecular drug delivery systems.

KEYWORDS: DNA, vector, degradable, supramolecular, self-assembly
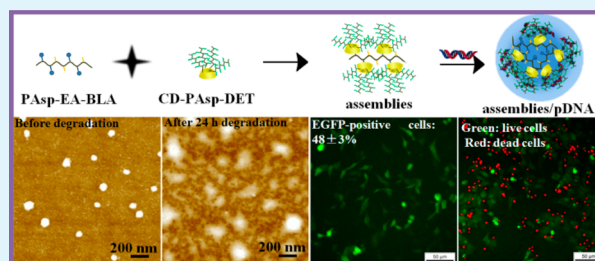
INTRODUCTION

Cancer is a generic group of diseases with four major characteristics of uncontrolled growth, invasion of adjacent tissue, metastasis, and immortality. The deaths caused by cancer are estimated to be around 12 million by 2030.[1] Gene therapy has attracted intense research interest as an effective way to treat cancers and even some genetic disorders. The crux of gene therapy is to design gene vectors with low cytotoxicity and effective transfection ability.[2,3] Cationic polymers used as nonviral vectors for delivering nucleic acids encompass a wide range of substances, such as polyethylenimine (PEI),[4] poly(2-(dimethyl amino)ethyl methacrylate),[4] poly(L-lysine),[5] poly-(aspartic acid) (PAsp),[6,7] polyamidoamine,[8] and cyclodextrin (CD)-based polycations.[9−11] Among them, PAsp-based nanoparticles,[12,13] micelles,[14−18] nanocapsules,[19] and membranes[20] had been proposed for the delivery of drug, DNA, RNA and proteins, because of their nontoxic, biocompatible, and biodegradable characteristics. It was reported that the modification of PAsp using diethylenetriamine (DET) could enhance the DNA-condensing ability, where DET has appreciably high buffering capacity and capability to disturb the cell membrane integrity at endosomal pH, facilitating the endosomal escape of the polycation/pDNA complexes.[6]

In addition to varied compositions, the structures of polycation vectors also play a significant role in facilitating gene delivery. Star-shaped, comb-shaped, or supramolecular assembly-based polycations have recently attracted considerable attention as effective gene carriers due to their dense molecular architecture and moderate flexibility.[21−23] CDs are a series of cyclic oligosaccharides composed of D(+)-glucose units, which could improve gene bioavailability via enhancing cell membrane absorption or stabilizing gene in physiological media.[24] A series of CD-cored star-shaped polycations were designed for the efficient delivery of nucleic acids.[25,26] Another advantage offered by CD is its easy self-assembly process with typical small hydrophobic molecules, such as benzene and adamantane, to produce supramolecular delivery systems.[27−31]

To construct better delivery systems, a series of new pseudocomb PAsp-based supramolecular assemblies were proposed in this work via the host−guest interactions between the α-CD or β-CD-cored PAsp-based star polycation hosts and the pendant benzene groups-containing PAsp backbone guests
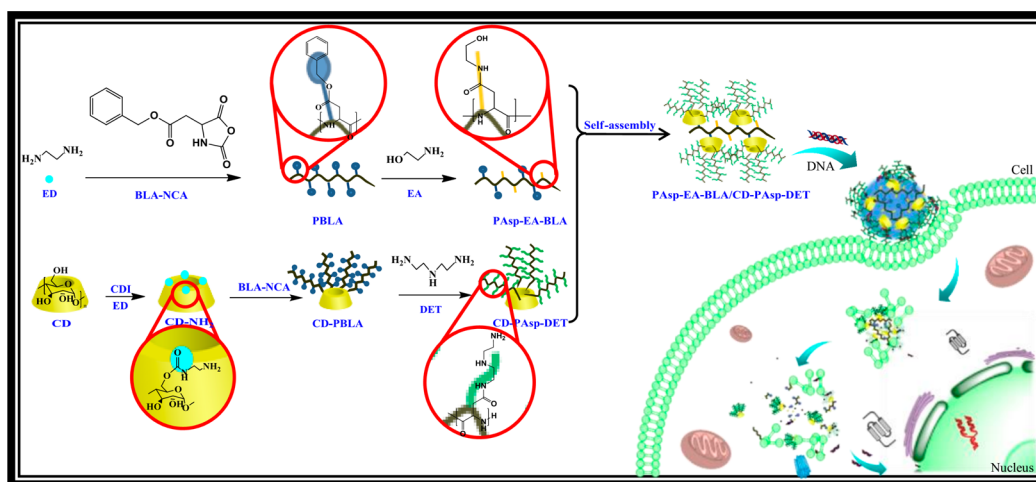
Figure 1. Schematic diagram illustrating the processes of preparation and cellular uptake of PAsp-EA-BLA/CD-PAsp-DET/pDNA nanocomplexes.

Table 1. Preparation and Characterization of Polymers

samples	[BLA-NCA]:[CD-NH$_2$] feed ratio	M_n (g/mol)[e]	PDI[e]
PAsp-EA-BLA[a]		7.50×10^3	1.25
α-CD-PBLA-1[b]	30:1	6.31×10^3	1.08
α-CD-PBLA-2[b]	45:1	9.58×10^3	1.07
α-CD-PBLA-3[b]	60:1	1.22×10^4	1.16
β-CD-PBLA-1[b]	30:1	6.35×10^3	1.12
β-CD-PBLA-2[b]	60:1	1.21×10^4	1.18
α-CD-PAsp-DET-1[c]		5.36×10^3	1.38
α-CD-PAsp-DET-2[c]		8.54×10^3	1.29
α-CD-PAsp-DET-3[c]		1.11×10^4	1.26
β-CD-PAsp-DET-1[c]		5.40×10^3	1.35
β-CD-PAsp-DET-2[c]		1.13×10^4	1.27
PAsp-EA-BLA/α-CD-PAsp-DET-1[d]		7.21×10^4	1.61
PAsp-EA-BLA/α-CD-PAsp-DET-2[d]		1.06×10^5	1.52
PAsp-EA-BLA/α-CD-PAsp-DET-3[d]		1.40×10^5	1.78
PAsp-EA-BLA/β-CD-PAsp-DET-1[d]		7.18×10^4	1.66
PAsp-EA-BLA/β-CD-PAsp-DET-2[d]		1.39×10^5	1.75

[a]Synthesized using a [BLA-NCA (1 g)]:[ED] feed ratio of 50:1 at 40 °C in 14 mL of DMF/CH$_2$Cl$_2$ (1/10, v/v) mixture for 48 h, followed with partial hydroxylation by adding EA for 24 h. [b]Synthesized using different [BLA-NCA (1 g)]:[CD-NH$_2$] feed ratios at 50 °C in 14 mL of DMSO for 72 h, where CD-NH$_2$ possessed four primary amine groups. [c]Synthesized by functionalizing CD-PBLA with excess DET. [d]Obtained by self-assembly of PAsp-EA-BLA and CD-PAsp-DETs. [e]Determined from GPC results. PDI = weight-average molecular weight/number-average molecular weight, or M_w/M_n.

(Figure 1). Such assemblies synergistically combined together the advantages of biodegradability of PAsp, low-cytotoxicity and flexibility of star polycation, and dynamic-tunable ability of supramolecular polymers. The PAsp-based assemblies were investigated in terms of degradability, pDNA-condensing capability, cytotoxicity, gene transfection, and in vitro antitumor effect using a suicide gene therapy system. The present work would provide a flexible approach for design of novel degradable supramolecular therapeutic delivery systems.

■ EXPERIMENTAL SECTION

Materials. Branched polyethylenimine (PEI, $M_w \sim 25\,000$ Da), 1,1′-carbonyldiimidazole (CDI, 97%), triphosgene (>99%), ethanolamine (EA, >98%), anhydrous dichloromethane (ultra drying, H$_2$O ≤ 0.004%), N-methyl-2-pyrrolidone (NMP, >98%), ethylenediamine (ED, >98%), diethylenetriamine (DET, >98%), calcium hydride (CaH$_2$, AR), 3-(4,5-dimethylthiazol-2-yl)-2,5-diphenyl tetrazolium bromide (MTT), fluorescein diacetate (FDA, >98%), propidium iodinate (PI, >98%), D-mannitol (>99%), penicillin, and streptomycin were obtained from Sigma-Aldrich Chemical Co., St. Louis, MO.

Anhydrous 1,4-dioxane L-aspartic acid β-benzyl ester (BLA, >98%), 5-fluorocytosine (5-FC, 98%), anhydrous dimethyl sulfoxide (DMSO), and anhydrous N,N-dimethylformamide (DMF) were purchased from Tokyo Chemical Industry Co. Ltd., Japan. Acetic ether and n-hexane were dried over CaH$_2$ for at least 1 week and were distilled over fresh CaH$_2$ powder under a normal pressure. Other solvents were directly used without treatment. HEK293 and HepG2 cell lines were purchased from the American Type Culture Collection (ATCC, Rockville, MD). Plasmid pRL-CMV encoding Renilla luciferase (Promega Co, Cergy Pontoise, France), plasmid pEGFP-N1encoding enhanced green fluorescent protein (EGFP) (BD Biosciences, San Jose, CA), and plasmid pAdTrack-CMV-CD (pCMVCD) encoding *Escherichia coli* cytosine deaminase (ECD) were amplified in *E. coli* and purified according to the supplier's protocol (Qiagen GmbH, Hilden, Germany).

Preparation of CD-NH$_2$. As shown in Figure 1, some hydroxyl groups of α-CD or β-CD were reacted with ED in the presence of CDI to produce the amine groups-terminated CDs (α-CD-NH$_2$ or β-CD-NH$_2$). Details on the preparation and characterization of β-CD-NH$_2$ with four primary amine groups were described in our previous work.[32] α-CD-NH$_2$ with four primary amine groups was prepared

using similar procedures. Briefly, a CDI solution (8.24 mmol in 6 mL of anhydrous DMSO) was added dropwise at ambient temperature into an α-CD solution (1.03 mmol in 4 mL of anhydrous DMSO). The CDI-activating reaction was allowed to proceed at room temperature for 4 h. Then, 2.4 mL of ED was added. The reaction mixture was stirred at room temperature for 48 h to produce α-CD-NH_2. The final reaction mixture was precipitated and washed with excess acetone, prior to being dissolved in 5 mL of deionized water and dialyzed against deionized water with dialysis membrane (MWCO, 1000 Da) at room temperature for 24 h. The final products were freeze-dried to produce about 0.55 g of α-CD-NH_2.

Synthesis of Linear and Star-shaped Poly(β-benzyl-L-aspartate). β-Benzyl-L-aspartate N-carboxy anhydride (BLA-NCA) was prepared using the Fuchs−Farthing method, through the reaction of BLA and triphosgene.[32,33] The detailed procedures are described earlier.[32] Poly(β-benzyl-L-aspartate) (PBLA) was synthesized by the ring-opening polymerization of BLA-NCA. Linear PBLA was obtained from ED initiation, whereas star-shaped PBLA (CD-PBLA) was obtained from α-CD-NH_2 or β-CD-NH_2 initiation. The polymerization reaction was performed under typical ring-opening conditions.[32] Briefly, 10 mL of BLA-NCA solution was added dropwise into 4 mL of initiator solution under a nitrogen atmosphere. For linear PBLA, 1 g of BLA-NCA (4.50 mmol) and 6 μL of ED (0.09 mmol) were dissolved in 10 and 4 mL of DMF/CH_2Cl_2 (1/10, v/v) mixture, respectively. The reaction solution was stirred for 2 days at 40 °C. For α-CD-cored PBLA (α-CD-PBLA), 1 g of BLA-NCA (4.50 mmol) was initiated by three different amounts of α-CD-NH_2 (namely 0.15, 0.10, and 0.075 mmol) in 14 mL of anhydrous DMSO at 50 °C for 3 days, resulting in α-CD-PBLA-1, α-CD-PBLA-2, and α-CD-PBLA-3, respectively. β-CD-PBLA-1 (corresponding to α-CD-PBLA-1) and β-CD-PBLA-2 (corresponding to α-CD-PBLA-3) were prepared by varying feed ratios of BLA-NCA/β-CD-NH_2 (Table 1). At the reaction end, the reaction solution was pulled into n-hexane. A white precipitate was obtained by centrifugation. The precipitate was washed by n-hexane twice before drying under vacuum.

Synthesis of Partially Hydroxylated PBLA. For the partial hydroxylation of PBLA, the molar feed ratio [BLA units of 0.5 g PBLA]:[EA] of 1:0.8 was used in 10 mL of anhydrous DMSO at room temperature for 1 day. The final reaction mixture was precipitated and washed with excess diethyl ether, prior to being dissolved in 10 mL of deionized water and dialyzed against deionized water (3 × 5 L) with dialysis membrane (MWCO, 3000 Da) at room temperature for 8 h. The final partial hydroxylated PBLA (PAsp-EA-BLA) was freeze-dried (about 0.25 g).

Synthesis of DET-Aminated Star PBLA. For the preparation of CD-cored DET-aminated PBLA (CD-PAsp-DET), β-CD-PBLA or α-CD-PBLA (0.5 g) and DET (8.14 mL, DET/BLA molar ratio = 50) were dissolved in 10 and 6 mL of NMP, respectively. Then the DET solution was added to the PBLA solution and the mixture was stirred vigorously at 4 °C for 1.5 h. The reaction mixture was neutralized with 62 mL of acetic acid aqueous solution (20 wt %) in an ice bath, followed by dialyzing against 0.01 M HCl and subsequently deionized water for 3 days[18] in prior to being freeze-dried.

Self-Assembly between PAsp-EA-BLA and CD-PAsp-DET. Supramolecular PAsp-EA-BLA/α-CD-PAsp-DETs or PAsp-EA-BLA/β-CD-PAsp-DETs was obtained by assembling PAsp-EA-BLA with α-CD-PAsp-DETs or β-CD-PAsp-DETs (Table 1), and the mechanism has been described earlier.[34] CD containing peculiar hydrophobic cavum could form inclusion complexes with various guest molecules. The PAsp-EA-BLA backbones contained many benzene rings that can be the hydrophobic sites to assemble with the CDs of CD-PAsp-DETs. With the 1:1 molar feed ratio of the CD (of CD-PAsp-DETs)/ benzene units (of PAsp-EA-BLA), a PAsp-EA-BLA solution (0.01 g in 1 mL of deionized water) was added dropwise at ambient temperature into the flasks containing 10 mL of α-CD-PAsp-DET or β-CD-PAsp-DET solution. The mixture was stirred for 4 h and then freeze-dried to yield PAsp-EA-BLA/α-CD-PAsp-DET or PAsp-EA-BLA/β-CD-PAsp-DET assemblies.

Material Characterization. The molecular weights of polymers were determined by gel permeation chromatography (GPC) and chemical structures by nuclear magnetic resonance (NMR) spectroscopy. GPC measurements of linear and star PBLAs were performed on a Waters GPC system equipped with Waters Styragel columns, a Waters-2487 dual wavelength (λ) UV detector, and a Waters-2414 refractive index detector. DMSO was used as the eluent at a low flow rate of 1.0 mL/min at 25 °C. GPC measurements of CD-PAsp-DETs were performed on a YL9100 GPC system equipped with a UV/vis detector and Waters Ultrahydrogel 250TM and Ultrahydrogel LinearTM 7.8 × 300 mm columns. A pH 3.5 acetic buffer solution was used as the eluent at a low flow rate of 0.5 mL/min at 25 °C. Monodispersed poly(ethylene glycol) standards were used to obtain a calibration curve. ^{1}H NMR spectra were measured by accumulation of 1000 scans at a relaxation time of 2 s on a Bruker ARX 300 MHz spectrometer, using D_2O or DMSO-d_6 as the solvent. For the biodegradation study, polymers were dissolved in acetic acid−sodium acetate buffer (pH = 5.8 PBS), and the solution was constantly shaken in a 37 °C incubator at 100 rpm. The molecular weights of degraded polymers were measured with GPC.

Biophysical Characterization. All polycation stock solutions were prepared in distilled water at a nitrogen concentration of 10 mM. Solutions were filtered through sterile membranes (0.2 μm) of average pore size and stored at 4 °C. Polycation-to-pDNA ratios are expressed as molar ratios of nitrogen (N) in polymers to phosphate (P) in DNA (or as N/P ratios). All polycation/pDNA complexes were formed by mixing equal volumes of polycation and pDNA solutions at the desired N/P ratios. Each mixture was vortexed and incubated for 30 min at room temperature. Polycations were examined for their ability to bind pDNA through agarose gel electrophoresis using the similar procedures as those described earlier.[21] The particle sizes and ζ-potentials of the polycation/pDNA complexes were measured in triplicate using a Zetasizer Nano ZS (Malvern Instruments, Southborough, MA).[21] The morphological structures of polycation/pDNA complexes before and after 24 h of degradation were visualized using an atomic force microscopy (AFM) system (Multimode 8, Bruker Daltonics Inc., Germany). The samples were imaged using the tapping mode with setting of 512 pixels/line and 0.9 Hz scan rate.

Cell Viability Assay. The cytotoxicity of polycations was evaluated in HEK293 and HepG2 cell lines using MTT assay. Details on the measurement were described in our previous work.[21] Briefly, the HEK293 or HepG2 cells were seeded into 96-well plates at a density of 10^4 cells/well and incubated. Then, the culture medium was replaced with various N/P ratios of polymer/pDNA complexes. Then, the cells were incubated with the addition of sterile-filtered MTT stock solution. The cytotoxicity of the materials was evaluated by the cell viability (%), which was calculated from $[A]_{test}/[A]_{control} \times 100\%$, where $[A]_{test}$ and $[A]_{control}$ are the absorbance values of the wells (with the polymers) and control ones (without the polymers), respectively. For each sample, the final viability was the average of those measured from six wells in parallel. The cell viability was also assessed in HepG2 cells using a rapid, simultaneous double-staining procedure of FDA and PI.[35] The detailed procedures were described earlier.[32] The stained cells were imaged using a Leica DMIL fluorescence microscope. FDA-stained living cells are in green and PI-stained dead cells are in red.

Transfection Assay. In vitro transfection assay was performed first using plasmid pRL-CMV as the reporter gene in HEK293 and HepG2 cell lines in fresh normal medium with 10% FBS.[21] Briefly, the cells were seeded in 24-well plates at a density of 5×10^4 cells in 500 μL of medium/well and incubated for 24 h. Then the complexes (20 μL/ well containing 1.0 μg of pDNA) at various N/P ratios were added to the transfection medium. Four hours later, the medium was replaced with 500 μL of the fresh normal medium (supplemented with 10% FBS) and incubated for an additional 20 h. Finally, the cultured cells were washed with PBS and lysed with lysis buffer. Luciferase gene expression was quantified using a commercial kit (Promega Co., CergyPontoise, France) and a luminometer (Berthold Lumat LB 9507, Berthold Technologies GmbH. KG, Bad Wildbad, Germany). Protein concentration in the cell samples was analyzed using a bicinchoninic acid assay (Biorad Lab, Hercules, CA). Gene expression results were expressed as relative light units (RLUs) per milligram of cell protein

lysate (RLU/mg protein). Gene transfection was also assessed at the optimal N/P ratios of polycations using plasmid pEGFP-N1 as the reporter gene in HepG2 cell lines. The transfected cells were imaged by using a Leica DMIL fluorescence microscope. The flow cytometry (FCM, Beckman Coulter, Pasadena, CA) was used to measure the percentage of EGFP-positive cells.

Cellular Internalization. HepG2 cells were used to evaluate the amount of cellular uptake. Briefly, 8×10^5 HepG2 cells/well were seeded into a 6-well plate and incubated for 24 h. Then, the medium was replaced with 2 mL of DMEM with 10% FBS. The vector materials were mixed with the fluorescent dye YOYO-1-labeled pDNA (pRL-CMV)[26] at the N/P ratio of 15. Thirty minutes later, the complexes were added to each well and incubated for 4 h. After washed with PBS, the cells were imaged by a Leica DMI3000 B fluorescence microscope[36] or trypsinized for flow cytometry assay (FACSCalibur).[26] Moreover, the cell nuclei were stained about 10 min with 150 ng/mL DAPI in PBS before fluorescence imaging.

In Vitro Antitumor Effect Using a 5-FC/ECD System. Suicide gene assay was performed in vitro using plasmid pCMVCD in HepG2 cell lines. The sensitivity of 5-FC was assessed using the similar procedures as those described earlier.[37] Briefly, HepG2 cells were seeded into a 96-well plate at a density of 6×10^3 cells per well and incubated for 24 h. At the time of transfection, the medium was replaced with 150 μL of fresh normal medium. The polycation/pDNA complexes at their optimal N/P ratios (10 μL/well containing 0.3 μg of pCMVCD) were added and incubated with the cells for 4 h under standard conditions. Then, the medium was replaced with 150 μL of the fresh normal medium, and 5-FC (0−160 μg/mL) was added subsequently. After 72 h of incubation, the cell viability was evaluated by MTT assay and FDA-PI double staining methods as described above.

Statistical Analysis. All experiments were repeated at least three times. Data are presented as means ± standard deviation. Statistical significance ($p < 0.05$) was evaluated by using Student's t-test when only two groups were compared.

■ RESULTS AND DISCUSSION

Synthesis of PAsp-based Vectors. The new PAsp-based supramolecular assemblies were prepared via the host−guest interactions. The synthetic routes of the PAsp-based star polycation hosts and the pendant benzene groups-containing PAsp backbone guests were illustrated in Figure 1. The linear and star PBLA polymers were first obtained via ring-opening polymerization of BLA-NCA initiated by primary amine groups of ED or CD-NH$_2$. In this work, in order to avoid potential gelation and introduce some flexibility onto the star polycations,[38] four hydroxyl groups of α-CD or β-CD were directly activated by CDI and converted into amine initiation sites for growing PBLA arms. The detailed characterization of β-CD-NH$_2$ was described in our previous work.[32] The typical ^{1}H NMR spectra of α-CD-NH$_2$ was shown and analyzed in details in the Supporting Information (Figure S1).

By using ED and CD-NH$_2$ initiators, the corresponding linear and star PBLA polymers were subsequently prepared under the typical polymerization of BLA-NCA. Linear PBLA was partially aminolyzed with ethanolamine (EA) to produce the pendant benzene groups-containing PAsp guests (PAsp-EA-BLA, 7.50×10^3 g/mol, PDI = 1.25, Table 1), where some benzyl ester pendant groups of PLBA were substituted by EA. The EA/benzene ratio of PAsp-EA-BLA was about 1.5. The residual benzene groups of PAsp-EA-BLA would be used for further assembly with CD-cored star PAsp polycations.

In this work, two kinds of star PBLAs (α-CD-PBLA and β-CD-PBLA) were prepared. The star PBLAs with different arm lengths were synthesized by varying the feed ratio of BLA-NCA/CD-NH$_2$. As shown in Table 1, the molecular weights of

α-CD-PBLAs are 6.31×10^3 (for α-CD-PBLA-1), 9.58×10^3 (for α-CD-PBLA-2), and 1.22×10^4 g/mol (for α-CD-PBLA-3), respectively. The prepared β-CD-PBLA-1 ($M_n = 6.35 \times 10^3$ g/mol) and β-CD-PBLA-2 ($M_n = 1.21 \times 10^4$ g/mol) are comparable to α-CD-PBLA-1 and α-CD-PBLA-3, respectively. The typical ^{1}H NMR spectrum of CD-PBLA was shown and analyzed in details in the Supporting Information (Figure S1). CD-PBLAs were subsequently aminolyzed with excess amounts of DET to produce the α-CD-PAsp-DET (or β-CD-PAsp-DET) vectors with flanking cationic amine groups (Figure 1), where benzyl ester pendant groups of CD-PBLA were substituted by DET units. The molecular weights of CD-PAsp-DETs are summarized in Table 1. The typical ^{1}H NMR spectrum of CD-PAsp-DET is shown and analyzed in detail in the Supporting Information (Figure S1).

With the 1:1 molar feed ratio of benzene groups/CD units, PAsp-EA-BLA was assembled with different multiple α-CD-PAsp-DETs (or β-CD-PAsp-DETs), producing five supramolecular assemblies, namely PAsp-EA-BLA/α-CD-PAsp-DET-1, PAsp-EA-BLA/α-CD-PAsp-DET-2, PAsp-EA-BLA/α-CD-PAsp-DET-3, PAsp-EA-BLA/β-CD-PAsp-DET-1, and PAsp-EA-BLA/β-CD-PAsp-DET-2 (Table 1). The typical ^{1}H NMR spectrum of PAsp-EA-BLA/CD-PAsp-DET is shown and analyzed in detail in the Supporting Information (Figure S1). Table 1 summarizes the GPC results of the PAsp-based supramolecular PAsp-EA-BLA/CD-PAsp-DETs. The supramolecular assemblies exhibited substantially higher molecular weights, indicating that PAsp-EA-BLA successfully assembled with CD-PAsp-DET.

Degradation of PAsp-based Vectors. The degradation of gene vectors plays an important role in the release of pDNA, regulating cytotoxicity of vectors and their final removal from the body. The degradable amide bonds of PAsp-based assemblies can be readily broken down in intracellular endosomal environment, which provided the degradability of the polymers. To demonstrate the degradation ability, α-CD-PAsp-DET-3 (with the starting $M_n \sim 5.36 \times 10^3$ g/mol, Table 1) and PAsp-EA-BLA/α-CD-PAsp-DET-3 (with the starting $M_n \sim 1.40 \times 10^5$ g/mol) were selected as the representatives to dissolve in acetic acid−sodium acetate buffer (pH = 5.8, analogous to endosomal environment) and kept in a 37 °C incubator. The solution was withdrawn at different time points. The molecular weights of degraded vectors were determined by GPC. As shown in Figure 2a, the M_n of PAsp-EA-BLA/α-CD-PAsp-DET-3 decreased significantly with degradation time especially in the first 10 days. On the other hand, the α-CD-PAsp-DET-3 degraded relatively slowly. Both CD-PAsp-DET hosts and PAsp-EA-BLA guests contained degradable amide bonds. Thus, the rapid degradation behaviors of the PAsp-EA-BLA/CD-PAsp-DET assemblies were arisen from their host and guest parts' degradation activities. The aqueous GPC traces of α-CD-PAsp-DET-3 before and after the final degradation also show the significant differences (Figure 2b). The M_n of the final degraded products was near that of α-CD, which was in the 10^3 orders of magnitude. The above results demonstrated the good degradation ability of PAsp-based assemblies.

Biophysical Properties of PAsp-based Vector/pDNA Complexes. In this work, agarose gel electrophoresis, particle size, and ζ-potential measurements were used to examine the condensation ability of PAsp-based vectors. The electrophoretic mobility of the polymer/pDNA complexes was first analyzed on an agarose gel at various N/P ratios. Figure 3 shows the gel retardation results of the different PAsp-based vector/pDNA
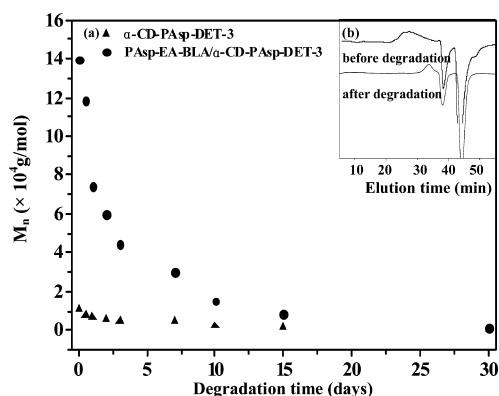
Figure 2. (a) Change of molecular weights of α-CD-PAsp-DET-3 and PAsp-EA-BLA/α-CD-PAsp-DET-3 with degradation time at 37 °C and (b) aqueous GPC traces obtained for α-CD-PAsp-DET-3 before and after degradation.
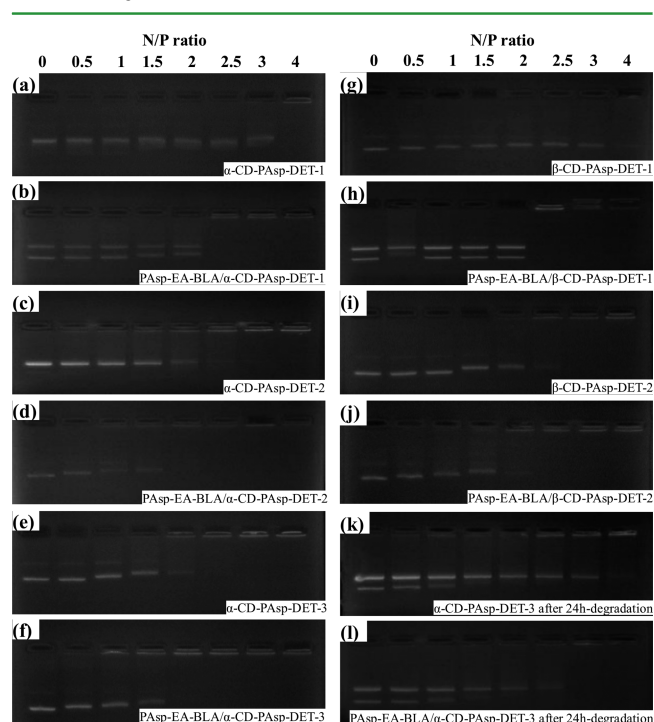

Figure 3. Electrophoretic mobility of pDNA in the complexes of CD-PAsp-DET, PAsp-EA-BLA/CD-PAsp-DET, α-CD-PAsp-DET-3 (after 24 h degradation at various N/P ratios), and PAsp-EA-BLA/α-CD-PAsp-DET-3 (after 24 h degradation at various N/P ratios).

As shown in Figure 2, the amide bonds in PAsp were readily degradable under an intracellular endosomal environment. The degradation would be beneficial to the release of pDNA from polymer/pDNA complexes. Such responsiveness can be evaluated by agarose gel retardation electrophoresis.[32] As shown in Figure 3k,l, after 24 h of degradation, the substantially increased mobility of the pDNA (as indicated by higher threshold N/P ratios) in the complexes was observed. The above results indicated that degradation of PAsp-based vectors could weaken pDNA condensation ability, which may facilitate the release of pDNA from the complexes in cells and, in turn, benefit the resultant gene expression.

The particle size and surface charge are the two important factors in modulating cell uptake of polymer/pDNA complexes. The particle sizes of the PAsp-based vector/pDNA complexes at various N/P ratios are shown in Figure 4a. All of the
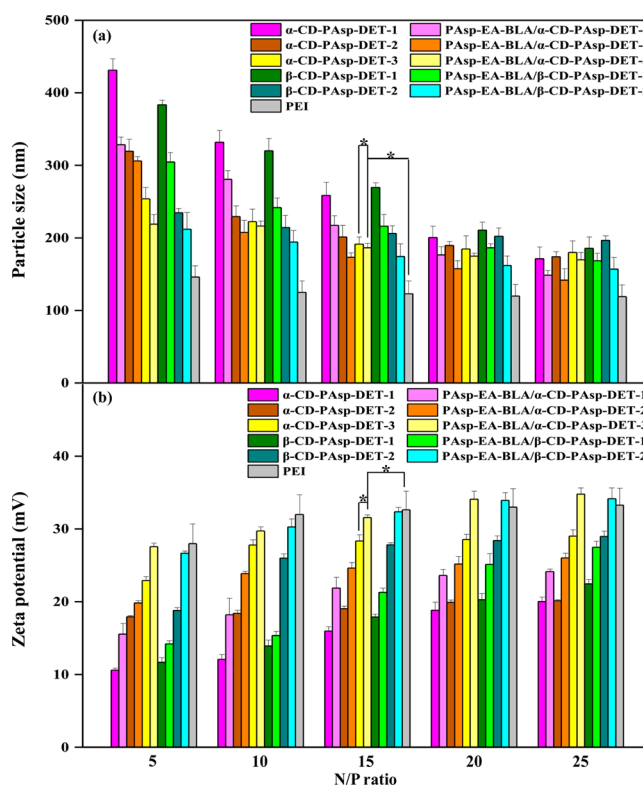

Figure 4. (a) Particle size and (b) ζ-potential of the pDNA complexes of CD-PAsp-DET, PAsp-EA-BLA/CD-PAsp-DET, and PEI (25 kDa) at various N/P ratios (*$p < 0.05$).

complexes. The mobility of the pDNA decreased with the increase of N/P ratio. The threshold N/P ratio (for completely compacting pDNA) indicates the pDNA-condensing ability. In general, higher-molecular-weight polycations exhibited higher condensation ability. With the increase in the length of PAsp-DET arms, CD-PAsp-DETs exhibited the decreased threshold N/P ratios, corresponding to their enhanced DNA-condensing abilities. For example, α-CD-PAsp-DET-3 and α-CD-PAsp-DET-1 retarded completely the migration of pDNA at the N/P ratios of 2.5 and 4, respectively. After self-assembly, the threshold N/P ratios of PAsp-EA-BLA/CD-PAsp-DETs were lower than the corresponding CD-PAsp-DETs (Figure 3). As shown in Table 1, PAsp-EA-BLA/CD-PAsp-DETs exhibited much higher molecular weights, resulting in a better pDNA-condensing ability.

complexes showed decreased particle sizes with increasing N/P ratios. Due to their lower pDNA-condensing ability, α-CD-PAsp-DET-1 and β-CD-PAsp-DET-1 condensed pDNA into larger aggregates at the low N/P ratio of 5. On the other hand, high-molecular-weight α-CD-PAsp-DET-3 and β-CD-PAsp-DET-2 condensed pDNA into smaller particles, especially at lower N/P ratios. Moreover, the particle sizes of supramolecular PAsp-EA-BLA/CD-PAsp-DET/pDNA complexes were smaller than those of their corresponding star CD-PAsp-DET/pDNA complexes at the same N/P ratio. These results corresponded to their different DNA-condensing ability (Figure 3). At N/P ratios of 10 and above, PAsp-EA-BLA/α-CD-PAsp-DET-3 and PAsp-EA-BLA/β-CD-PAsp-DET-2 condensed pDNA into particles within a diameter range of 200 nm. Such complexes can readily undergo endocytosis and facilitate

cell uptake.[39] The polydispersity index of all the complexes was between 0.1 and 0.2, indicating a low-to-moderate size distribution.[21] The ζ-potential of polymer/pDNA complexes was an indicator of surface charges on the complexes. As indicated in Figure 4b, the surface charges of the complexes became positive at N/P ratios of 5 and above. With the increase of the N/P ratio, their ζ-potentials increased slowly. The ζ-potentials of the PAsp-EA-BLA/α-CD-PAsp-DET-3 and PAsp-EA-BLA/β-CD-PAsp-DET-2 assemblies were comparable to those of PEI complexes. The positive net surface charges would produce good affinity for cell membrane and facilitate cell uptake.

The structures of PAsp-based vector/pDNA complexes were further explored by AFM. Before degradation, α-CD-PAsp-DET-3 (Figure 5a) and PAsp-EA-BLA/α-CD-PAsp-DET-3
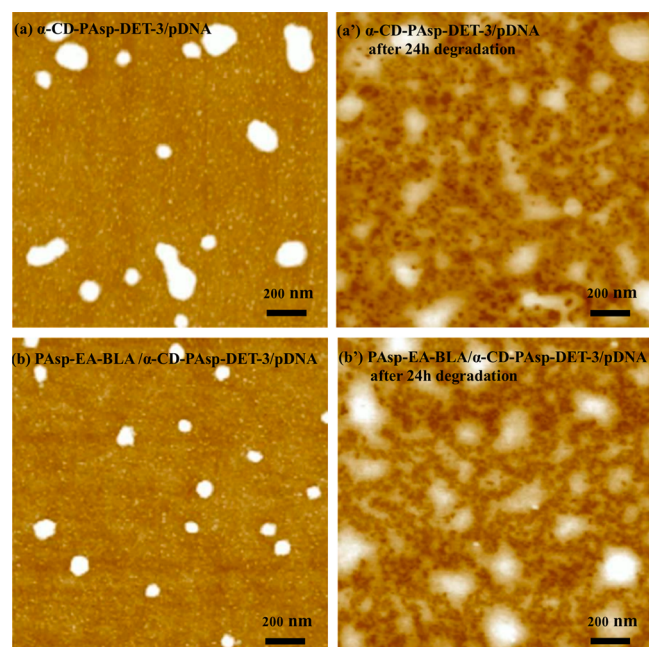

Figure 5. AFM images of α-CD-PAsp-DET-3/pDNA complex before (a) and after (a′) degradation, and of PAsp-EA-BLA/α-CD-PAsp-DET-3/pDNA complex before (b) and after (b′) degradation at the N/P ratio of 15.

(Figure 5b) can tightly compact pDNA to generate spherical nanoparticles. Moreover, the PAsp-EA-BLA/α-CD-PAsp-DET-3/pDNA complex exhibited a smaller size, consistent with its higher condensation ability (Figure 3f). After degradation in acetic acid−sodium acetate buffer (pH = 5.8), the complexes smashed to pieces (Figure 5a′,b′), indicating that degradation of PAsp-based vectors could benefit the intracellular release of pDNA from complexes.

Cell Viability Assay. High transfection efficiency and low toxicity should be balanced in a successful delivery system. The cell viability of the PAsp-based vector/pDNA complexes as a function of N/P ratio was evaluated in the HEK293 and HepG2 cells with MTT assay (Figure 6). All of the vectors exhibited a dose-dependent cytotoxicity effect. The cell viability decreased with the increase of N/P ratio. For CD-PAsp-DETs, the cytotoxicity slightly increased with the increase of the PAsp-DET arm length. The cytotoxicity of polycations increases with the molecular weight.[32] Compared with the control "gold-standard" PEI (25 kDa), CD-PAsp-DETs exhibited much lower
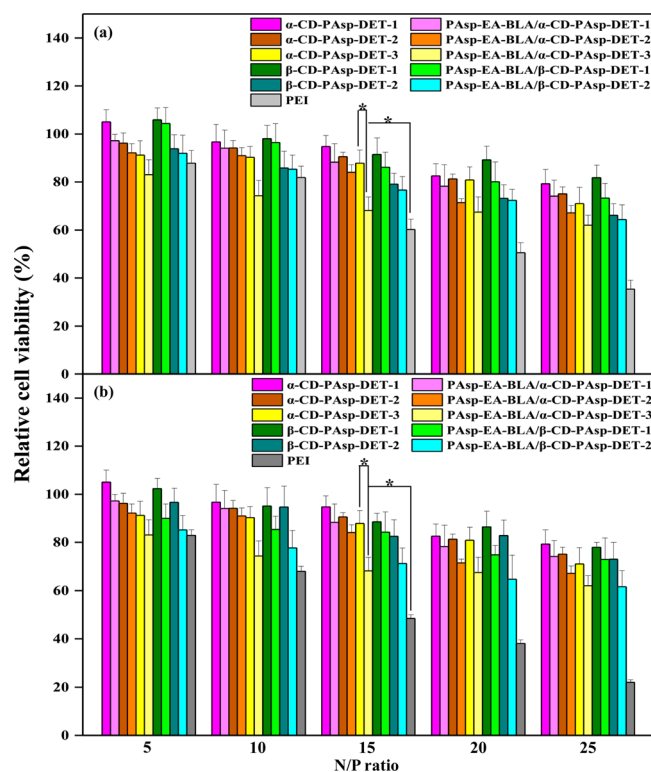

Figure 6. Cell viability assay in (a) HEK293 and (b) HepG2 cell lines with various N/P ratios of CD-PAsp-DET/pDNA, PAsp-EA-BLA/CD-PAsp-DET/pDNA, and PEI/pDNA (25 kDa). Cell viability was determined by the MTT assay and expressed as a percentage of the control cell culture ($*p < 0.05$).

cytotoxicity at the same N/P ratio, which could be attributed to nontoxic CD cores, the biocompatibility and degradability of PAsp arms, and the favorable property of star-shaped structure.[32] Supramolecular PAsp-EA-BLA/CD-PAsp-DETs showed slightly lower cell viabilities as compared with α-PAsp-DETs and β-PAsp-DETs, due to their high molecular weights and resultant high surface charges of pDNA complexes (Figure 4b). However, supramolecular PAsp-EA-BLA/CD-PAsp-DETs still exhibited significantly lower cytotoxicity (for example, at N/P = 20, cell viability > 70%) than the control PEI. The degradability of PAsp endows the supramolecular PAsp-EA-BLA/CD-PAsp-DETs with the favorable low toxicity, despite of their high molecular-weights. It was also noted that there was no obvious cytotoxicity difference between α-PAsp-DETs and β-PAsp-DETs (or PAsp-EA-BLA/α-PAsp-DETs and PAsp-EA-BLA/β-PAsp-DETs) of similar molecular weights.

To further show the lower cytotoxicity of degradable gene vectors over PEI (25 kDa), direct visualization of cell viability was also observed using a simultaneous double-staining procedure of FDA and PI. Figure 7 shows the representative images of HepG2 cells treated with the α-PAsp-DET-1/pDNA, PAsp-EA-BLA/α-PAsp-DET-1/pDNA, α-PAsp-DET-3/pDNA, PAsp-EA-BLA/α-PAsp-DET-3/pDNA complexes at the N/P ratio of 15, and the PEI/pDNA complex. FDA-stained living cells are in green and PI stained dead cells are in red. In comparison with PEI treatment, a significantly higher percentage of living cells were observed for PAsp-based vectors. The above results also suggested that PAsp-based vectors exhibited significantly lower cytotoxicity, which was consistent with the results of MTT assay (Figure 6).
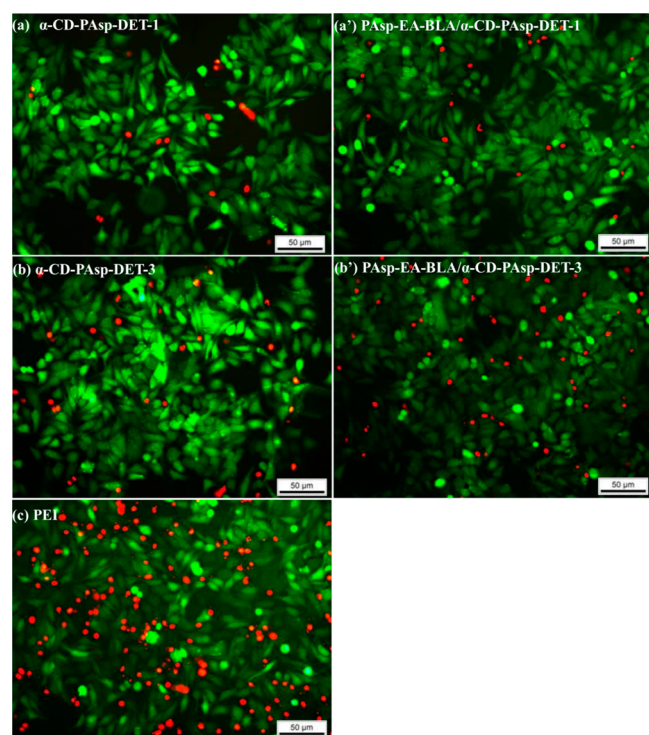
Figure 7. FDA-PI staining mediated by (a) α-CD-PAsp-DET-1/pDNA, (a′) PAsp-EA-BLA/α-CD-PAsp-DET-1/pDNA, (b) α-CD-PAsp-DET-3/pDNA, (b′) PAsp-EA-BLA/α-CD-PAsp-DET-3/pDNA, and (c) PEI/pDNA at the N/P ratio of 15 in HepG2 cells.
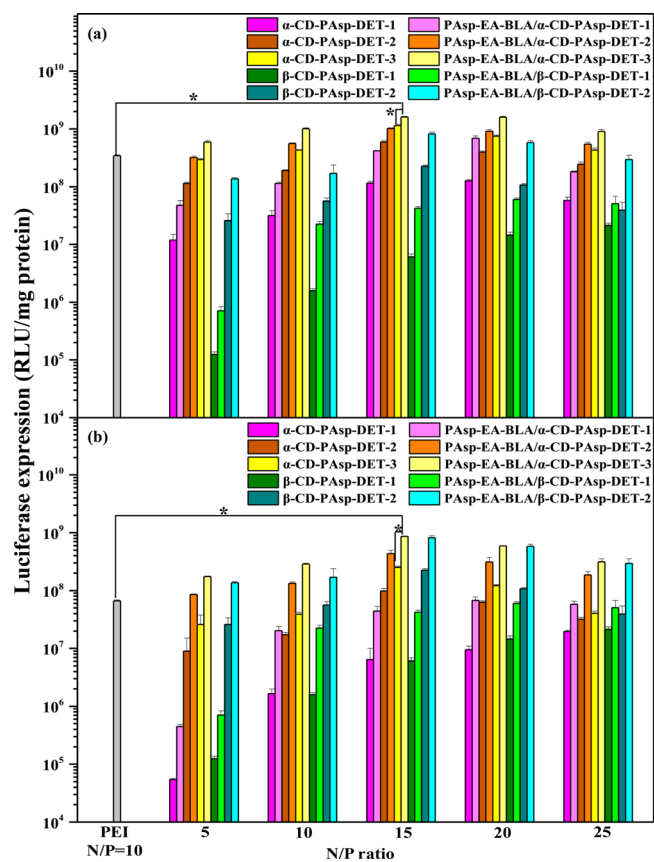

Figure 8. In vitro gene transfection efficiencies mediated by CD-PAsp-DET and PAsp-EA-BLA/CD-PAsp-DET at various N/P ratios in comparison those of PEI (25 kDa) at its optimal N/P ratio of 10 in (a) HEK293 and (b) HepG2 cell lines (*$p < 0.05$).

In Vitro Gene Transfection Assay. The in vitro gene transfection efficiency of the PAsp-based vector/pDNA complexes was evaluated by luciferase protein expression assay with pRL-CMV plasmid in HEK293 and HepG2 cell lines. Figure 8 shows the gene transfection efficiencies mediated by PAsp-based vectors at various N/P ratios in comparison with those of the control PEI (25 kDa) at its optimal N/P ratio of 10.[21−23] For CD-PAsp-DETs, the transfection efficiencies mediated by low-molecular-weight α-CD-PAsp-DET-1 (or β-CD-PAsp-DET-1) were significantly lower than those mediated by high-molecular-weight α-CD-PAsp-DET-3 (or β-CD-PAsp-DET-2). The transfection efficiencies mediated by PAsp-based vectors were dependent on the molecular weight. Higher-molecular-weight vectors possessed better binding ability and stability of complexes, probably leading to higher transfection efficiencies. Supramolecular PAsp-EA-BLA/CD-PAsp-DETs showed significantly higher transfection efficiencies than the corresponding CD-PAsp-DET counterparts. Supramolecular structure resulted in high-molecular-weight assemblies (Table 1), better DNA-condensing ability (Figure 3), and smaller particle sizes of complexes (Figure 4). In addition, supramolecular PAsp-EA-BLA/PAsp-DETs also possessed good degradability (Figures 2 and 3), which could benefit the intracellular release of pDNA from complexes and produce good gene transfection efficiencies.

In this study, it was found that the different kinds of CD-PAsp-DETs of similar molecular weights (namely, α-CD-PAsp-DET-1 vs β-CD-PAsp-DET-1, and α-CD-PAsp-DET-3 vs β-CD-PAsp-DET-2) possessed similar transfection efficiencies (accompanied by similar cell viabilities, as shown in Figure 6). The corresponding supramolecular PAsp-EA-BLA/α-CD-PAsp-DETs and PAsp-EA-BLA/β-CD-PAsp-DETs of similar molecular weights also possessed similar high transfection efficiencies (accompanied by similar DNA-condensing abilities, Figure 3). The above results indicated that types of CD cores have little effect on the gene transfection behaviors of star PAsp vectors. Both α-CD and β-CD can form supramolecular structures with benzene units in a PAsp backbone, which were stable enough to construct high-molecular-weight PAsp-based assemblies for efficient gene delivery.

By using plasmid pEGFP-N1, direct visualization of EGFP expression was performed in difficult-to-transfect HepG2 cells under fluorescence microscopy to further verify the gene delivery capability. Figure 9 shows the representative images of EGFP gene expression mediated by α-PAsp-DET-1, PAsp-EA-BLA/α-PAsp-DET-1, α-PAsp-DET-3, and PAsp-EA-BLA/α-PAsp-DET-3 at their respective optimal ratios. The EGFP-positive HepG2 cells were observed in green fluorescence. Supramolecular PAsp-EA-BLA/α-PAsp-DET-1 and PAsp-EA-BLA/α-PAsp-DET-3 mediated rather higher EGFP gene expression than their corresponding α-PAsp-DET-1 and α-PAsp-DET-3 counterparts. The percentages of the EGFP-positive HepG2 cells for α-CD-PAsp-DET-1, PAsp-EA-BLA/α-CD-PAsp-DET-1, α-CD-PAsp-DET-3 and PAsp-EA-BLA/α-CD-PAsp-DET-3 were 3%, 9%, 25%, and 48%, respectively, where PAsp-EA-BLA/α-PAsp-DET-3 exhibited the best gene transfection results. The above results were consistent with those of the luciferase expression (Figure 8). All the transfection results confirmed that the gene transfection ability
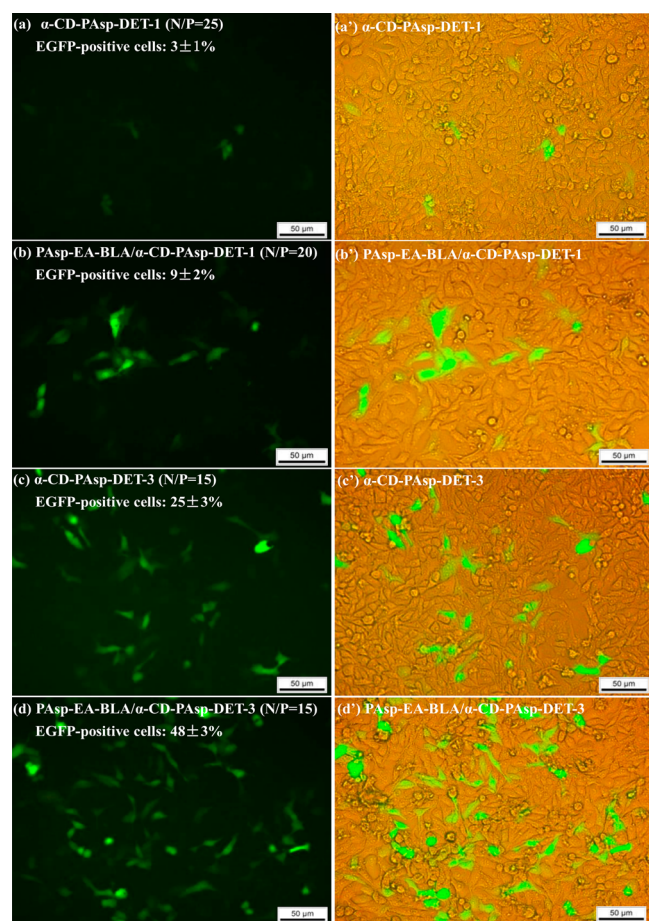
Figure 9. EGFP expression mediated by (a, a′) α-CD-PAsp-DET-1, (b, b′) PAsp-EA-BLA/α-CD-PAsp-DET-1, (c, c′) α-CD-PAsp-DET-3, and (d, d′) PAsp-EA-BLA/α-CD-PAsp-DET-3 at their respective optimal N/P ratios in HepG2 cell line.

could be improved by assembling star CD-PAsp-DETs with PAsp backbones.

In addition, it should be noted that with the increase of extracellular degradation time, the decreased molecular weight of the PAsp-based polycations led to lower transfection. However, for the transfection process, in the first 4 h of phagocytosis, the degradation of the PAsp-based polycations

was not obvious (as shown in Figure 2), and in the following 20 h, the vectors obtained obvious degradation, which benefited the release of the pDNA and resulted in high transfection. In the transfection process, the degradation of the freshly prepared PAsp-based polycations mainly took place inside the cells.

Cellular Internalization. As shown in Figures 8 and 9, α-PAsp-DET-3 and PAsp-EA-BLA/α-PAsp-DET-3 exhibited better transfection efficiencies among their corresponding CD-PAsp-DET and PAsp-EA-BLA/CD-PAsp-DET counterparts. Thus, the α-CD-PAsp-DET-3/pDNA and PAsp-EA-BLA/α-CD-PAsp-DET-3/pDNA complexes at their optimal N/P ratio of 15 were selected to study cellular internalization in HepG2 cell lines by fluorescence imaging and flow cytometry, where the pDNA was labeled with YOYO-1. Figure 10 shows the fluorescent images of HepG2 cells treated with the complexes after incubation for 4 h. The YOYO-1-labeled pDNA was shown in green and the DAPI-labeled nucleus was shown in blue. It was clearly observed that the amount of aggregation of the PAsp-EA-BLA/α-CD-PAsp-DET-3/pDNA complexes within the cells was higher than that of the α-CD-PAsp-DET-3/pDNA complexes. By measuring the percentage of fluorescence associated with the positive cells, the cellular uptakes of the complexes were evaluated by the flow cytometry assay. The PAsp-EA-BLA/α-CD-PAsp-DET-3/pDNA complexes showed the internalization rate of 88 ± 4%, in comparison with that (71 ± 2%) of α-CD-PAsp-DET-3/pDNA complexes. Such results were consistent with their respective condensation ability (Figure 3), particle size and ζ-potential (Figure 4). These positive factors may work together to facilitate the cellular uptake, and benefit the resultant gene delivery.

In Vitro Antitumor Effect with a 5-FC/ECD System. The 5-fluorocytosine (5-FC)/*E. coli* cytosine deaminase (ECD) system is a typical suicide gene therapy system for malignant tumors.[40] Positive cells with expression of ECD gene produce an enzyme that catalyzes the deamination of the nontoxic prodrug 5-FC to be the cytotoxic drug 5-fluorouracil (5-FU), resulting in tumor cell death. Due their higher gene transfection efficiencies, α-CD-PAsp-DET-3 and PAsp-EA-BLA/α-CD-PAsp-DET-3 were selected for treating cells with the 5-FC/ECD system. The antitumor effect was first evaluated at various 5-FC concentrations in HepG2 cells using MTT assay. As shown in Figure 11a, the cells treated with 5-FC alone were
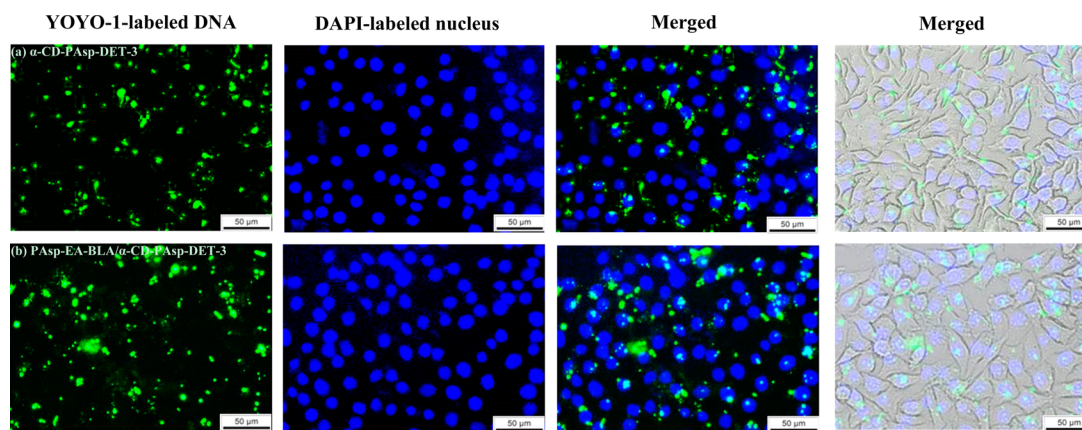

Figure 10. Fluorescent images of HepG2 cells treated with (a) α-CD-PAsp-DET-3/pDNA complexes and (b) PAsp-EA-BLA/α-CD-PAsp-DET-3/pDNA complexes at the N/P ratio of 15 for 4 h, where the YOYO-1-labeled pDNA is shown in green and the DAPI-labeled nucleus is shown in blue.
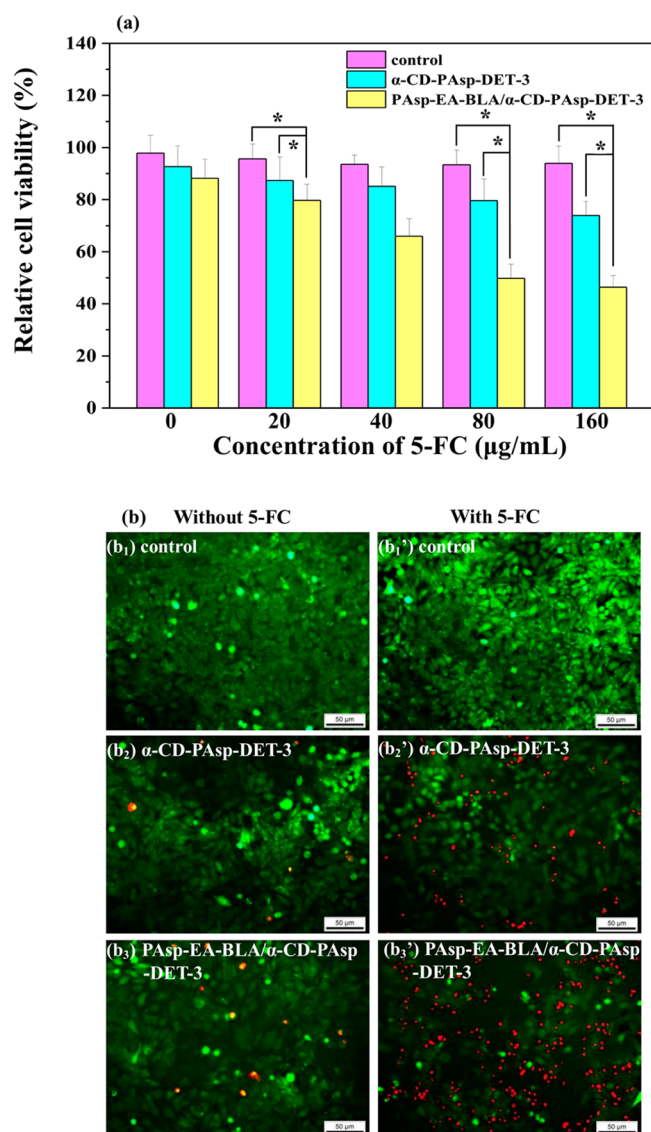
Figure 11. (a) Cell viability of the HepG2 cells treated with α-CD-PAsp-DET-3/pCMVCD and PAsp-EA-BLA/α-CD-PAsp-DET-3/pCMVCD complexes (at their optimal N/P ratios) under various 5-FC concentrations and (b) the corresponding FDA-PI staining in the absence (b_1, b_2, b_3) and presence of 5-FC of 80 μg/mL (b_1', b_2', b_3') (*$p < 0.05$).

taken as the control. The HepG2 cells treated by the α-PAsp-DET-3/pCMVCD and PAsp-EA-BLA/α-PAsp-DET-3/pCMVCD complexes showed obvious decrease in cell viability with the increase of 5-FC concentration, indicating that sufficient 5-FC was required for the 5-FC/ECD system to sustain effective abilities to kill tumor cells. Due to its higher gene delivery performance, the supramolecular PAsp-EA-BLA/α-CD-PAsp-DET-3 assembly showed lower cell viability than α-CD-PAsp-DET-3 at all 5-FC concentrations.

To further confirm the antitumor effect of the 5-FC/ECD system mediated by PAsp-based vectors, FDA-PI staining was used to directly visualize cell viability. Figure 11b shows the representative images of HepG2 cells treated by the α-CD-PAsp-DET-3/pDNA and PAsp-EA-BLA/α-CD-PAsp-DET-3/pDNA complexes. No obvious red (dead) cells were observed in the control groups without (Figure 11b_1) and with (Figure 11b_1') the 5-FC concentration of 80 μg/mL, indicating that the

cytotoxicity of the pro-drug 5-FC was neglectable in HepG2 cells. In the absence of 5-FC (Figure 11b_2,b_3), quite a few dead cells treated by PAsp-based vectors were observed, which was consistent with the low cytotoxicity of α-CD-PAsp-DET-3 and PAsp-EA-BLA/α-CD-PAsp-DET-3 (Figure 6). However, in the presence of 5-FC, a significant number of dead cells were observed (Figure 11b_2',b_3'), and more dead cells were observed for the treatment group of PAsp-EA-BLA/α-CD-PAsp-DET-3. The above results further confirmed the effective antitumor ability of the 5-FC/ECD system mediated by PAsp-EA-BLA/α-CD-PAsp-DET-3.

CONCLUSIONS

A series of new degradable supramolecular PAsp-EA-BLA/CD-PAsp-DET assemblies were successfully prepared via the host–guest interactions between the CD-cored PAsp-based polycations and the pendant benzene groups-containing PAsp backbones. PAsp-EA-BLA/CD-PAsp-DETs exhibited good degradability and low cytotoxicity. In comparison with CD-PAsp-DET counterparts, PAsp-EA-BLA/CD-PAsp-DET assemblies demonstrated the enhanced pDNA condensation abilities and much higher gene transfection efficiencies. It was also found that the types of CD cores had little effect on the gene transfection behaviors of star PAsp vectors. In addition, PAsp-EA-BLA/PAsp-DETs also possessed the effective antitumor ability by using the 5-FC/ECD gene therapy system. Such PAsp-based supramolecular assemblies would offer a new strategy for designing novel-structured degradable gene/drug delivery vectors.

ASSOCIATED CONTENT

Supporting Information

Representative structures of α-CD-NH$_2$ in D$_2$O, PAsp-EA-BLA in DMSO-d_6, α-CD-PAsp-DET-3 and PAsp-EA-BLA/α-CD-PAsp-DET-3 in D$_2$O characterized by ^{1}H NMR spectra (Figure S1). This material is available free of charge via the Internet at http://pubs.acs.org.

AUTHOR INFORMATION

Corresponding Authors
*E-mail: xufj@mail.buct.edu.cn (F.-J. Xu).
*E-mail: chendafu@jsthospital.org (D.-F. Chen).
Author Contributions
[⊥]These authors contributed equally to this work.
Notes
The authors declare no competing financial interest.

ACKNOWLEDGMENTS

REFERENCES

(1) Hunt, K. K.; Vorburger, S. A. Gene Therapy: Hurdles and Hopes for Cancer Treatment. *Science* 2002, 297, 415−416.
(2) De Smedt, S. C.; Demeester, J.; Hennink, W. E. Cationic Polymer based Gene Delivery Systems. *Pharm. Res.* 2000, 17, 113−126.
(3) Yudovin-Farber, I.; Domb, A. J. Cationic Polysaccharides for Gene Delivery. *Mater. Sci. Eng., C* 2007, 27, 595−598.

(4) Xu, F. J.; Yang, W. T. Polymer Vectors *via* Controlled/Living Radical Polymerization for Gene Delivery. *Prog. Polym. Sci.* **2011**, *36*, 1099−1131.

(5) Zauner, W.; Ogris, M.; Wagner, E. Polylysine-based Transfection Systems Utilizing Receptor-Mediated Delivery. *Adv. Drug Delivery Rev.* **1998**, *30*, 97−113.

(6) Uchida, H.; Miyata, K.; Oba, M.; Ishii, T.; Suma, T.; Itaka, K.; Nishiyama, N.; Kataoka, K. Odd-Even Effect of Repeating Amino-ethylene Units in the Side Chain of N-Substituted Polyaspartamides on Gene Transfection Profiles. *J. Am. Chem. Soc.* **2011**, *133*, 15524−15532.

(7) Zhu, Y.; Tang, G. P.; Xu, F. J. Efficient Poly(N-3-hydroxypropyl)-aspartamide-based Carriers *via* ATRP for Gene Delivery. *ACS Appl. Mater. Interfaces* **2013**, *5*, 1840−1848.

(8) Kukowska-Latallo, J. F.; Bielinska, A. U.; Johnson, J.; Spindler, R.; Tomalia, D. A.; Baker, J. R. Efficient Transfer of Genetic Material into Mammalian Cells Using Starburst Polyamidoamine Dendrimers. *Proc. Natl. Acad. Sci. U. S. A.* **1996**, *93*, 4897−4902.

(9) Azzam, T.; Raskin, A.; Makovitzki, A.; Brem, H.; Vierling, P.; Lineal, M.; Domb, A. J. Cationic Polysaccharides for Gene Delivery. *Macromolecules* **2002**, *35*, 9947−9953.

(10) Yang, C.; Li, H. Z.; Goh, S. H.; Li, J. Cationic Star Polymers Consisting of α-Cyclodextrin Core and Oligoethylenimine Arms as Nonviral Gene Delivery Vectors. *Biomaterials* **2007**, *28*, 3245−3254.

(11) Davis, M. E.; Brewste, M. E. Cyclodextrin-based Pharmaceutics: Past, Present and Future. *Nat. Rev. Drug Discovery* **2004**, *3*, 1023−1035.

(12) Lee, H. J.; Bae, Y. S. Cross-linked Nanoassemblies from Poly(ethylene glycol)-Poly(aspartate) Block Copolymers as Stable Supramolecular Templates for Particulate Drug Delivery. *Biomacromolecules* **2011**, *12*, 2686−2696.

(13) Suma, T.; Miyata, K.; Anraku, Y.; Watanabe, S.; Christie, R. J.; Takemoto, H.; Shioyama, M.; Gouda, N.; Ishii, T.; Nishiyama, N.; Kataoka, K. Smart Multilayered Assembly for Biocompatible siRNA Delivery Featuring Dissolvable Silica, Endosome-Disrupting Polycation, and Detachable PEG. *ACS Nano* **2012**, *6*, 6693−6705.

(14) Gao, H. J.; Xiong, J.; Cheng, T. J.; Liu, J. J.; Chu, L. P.; Liu, J. F.; Ma, R. J.; Shi, L. Q. *In Vivo* Biodistribution of Mixed Shell Micelles with Tunable Hydrophilic/Hydrophobic Surface. *Biomacromolecules* **2013**, *14*, 460−467.

(15) Takae, S.; Miyata, K.; Oba, M.; Ishii, T.; Nishiyama, N.; Itaka, K.; Yamasaki, Y.; Koyama, H.; Kataoka, K. PEG-Detachable Polyplex Micelles Based on Disulfide-Linked Block Catiomers as Bioresponsive Nonviral Gene Vectors. *J. Am. Chem. Soc.* **2008**, *130*, 6001−6009.

(16) Sanada, Y.; Akiba, I.; Hashida, S.; Sakurai, K. Composition Dependence of the Micellar Architecture Made from Poly(ethylene glycol)-block-Poly(partially benzyl-esterified aspartic acid). *J. Phys. Chem. B* **2012**, *116*, 8241−8250.

(17) Park, J. S.; Akiyama, Y.; Yamasaki, Y.; Kataoka, K. Preparation and Characterization of Polyion Complex Micelles with a Novel Thermosensitive Poly(2-isopropyl-2-oxazoline) Shell *via* the Complexation of Oppositely Charged Block Ionomers. *Langmuir* **2007**, *23*, 138−146.

(18) Diezi, T. A.; Bae, Y.; Kwon, G. S. Enhanced Stability of PEG-block-Poly(N-hexyl stearate L-aspartamide) Micelles in the Presence of Serum Proteins. *Mol. Pharmaceutics* **2010**, *7*, 1355−1360.

(19) Dong, W. F.; Kishimura, A.; Anraku, Y.; Chuanoi, S.; Kataoka, K. Monodispersed Polymeric Nanocapsules: Spontaneous Evolution and Morphology Transition from Reducible Hetero-PEG PIC Micelles by Controlled Degradation. *J. Am. Chem. Soc.* **2009**, *131*, 3804−3805.

(20) Kaneko, T.; Tanaka, S.; Ogura, A.; Akashi, M. Tough, Thin Hydrogel Membranes with Giant Crystalline Domains Composed of Precisely Synthesized Macromolecules. *Macromolecules* **2005**, *38*, 4861−4867.

(21) Xu, F. J.; Zhang, Z. X.; Ping, Y.; Li, J.; Kang, E. T.; Neoh, K. G. Star-shaped Cationic Polymers by Atom Transfer Radical Polymerization from β-Cyclodextrin Cores for Nonviral Gene Delivery. *Biomacromolecules* **2009**, *10*, 285−293.

(22) Xu, F. J.; Ping, Y.; Ma, J.; Tang, G. P.; Yang, W. T.; Kang, E. T.; Neoh, K. G. Comb-Shaped Copolymers Composed of Hydroxypropyl Cellulose Backbones and Cationic Poly((2-dimethylamino)ethyl methacrylate) Side Chains for Gene Delivery. *Bioconjugate Chem.* **2009**, *20*, 1449−1458.

(23) Wang, Z. H.; Zhu, Y.; Chai, M. Y.; Yang, W. T.; Xu, F. J. Biocleavable Comb-shaped Gene Carriers from Dextran Backbones with Bioreducible ATRP Initiation Sites. *Biomaterials* **2012**, *33*, 1873−1883.

(24) Mellet, C. O.; Fernándezb, J. M. G.; Benito, J. M. Cyclodextrin-based Gene Delivery Systems. *Chem. Soc. Rev.* **2011**, *40*, 1586−1608.

(25) Li, W. Y.; Chen, L. N.; Huang, Z. X.; Wu, X. F.; Zhang, Y. F.; Hua, Q. L.; Wang, Y. X. The Influence of Cyclodextrin Modification on Cellular Uptake and Transfection Efficiency of Polyplexes. *Org. Biomol. Chem.* **2011**, *9*, 7799−7806.

(26) Hu, Y.; Yuan, W.; Zhao, N. N.; Ma, J.; Yang, W. T.; Xu, F. J. Supramolecular Pseudo-Block Gene Carriers Based on Bioreducible Star Polycations. *Biomaterials* **2013**, *34*, 5411−5422.

(27) Zhang, J. X.; Sun, H. L.; Ma, P. X. Host-Guest Interaction Mediated Polymeric Assemblies: Multifunctional Nanoparticles for Drug and Gene Delivery. *ACS Nano* **2010**, *4*, 1049−1059.

(28) Miyauchi, M.; Harada, A. Construction of Supramolecular Polymers with Alternating α-, β-Cyclodextrin Units Using Conformational Change Induced by Competitive Guests. *J. Am. Chem. Soc.* **2004**, *126*, 11418−11419.

(29) Hu, Y.; Chai, M. Y.; Yang, W. T.; Xu, F. J. Supramolecular Host−Guest Pseudocomb Conjugates Composed of Multiple Star Polycations Tied Tunably with a Linear Polycation Backbone for Gene Transfection. *Bioconjugate Chem.* **2013**, *24*, 1049−1056.

(30) Dong, R. J.; Zhou, L. Z.; Wu, J. L.; Tu, C. L.; Su, Y.; Zhu, B. S.; Gu, H. C.; Zhu, X. Y. A Supramolecular Approach to the Preparation of Charge-tunable Dendritic Polycations for Efficient Gene Delivery. *Chem. Commun.* **2011**, *47*, 5473−5475.

(31) Harada, A.; Takashima, Y.; Yamaguchi, H. Cyclodextrin-based Supramolecular Polymers. *Chem. Soc. Rev.* **2009**, *38*, 875−882.

(32) Dou, X. B.; Hu, Y.; Zhao, N. N.; Xu, F. J. Different Types of Degradable Vectors from Low-Molecular-Weight Polycation-Functionalized Poly(aspartic acid) for Efficient Gene Delivery. *Biomaterials* **2014**, *9*, 3015−3026.

(33) Poché, D. S.; Moore, M. J.; Bowles, J. L. An Unconventional Method for Purifying the N-carboxyanhydride Derivatives of γ-Alkyl-L-Glutamates. *Synth. Commun.* **1999**, *29*, 843−854.

(34) Cramer, F.; Saenger, W.; Spatz, H. C. Inclusion Compounds. XIX.[la] The Formation of Inclusion Compounds of α-cyclodextrin in Aqueous Solutions. Thermodynamics and Kinetics. *J. Am. Chem. Soc.* **1967**, *89* (1), 14−20.

(35) Jones, K. H.; Senft, J. A. An Improved Method to Determine Cell Viability by Simultaneous Staining with Fluorescein Diacetate-Propidium Iodide. *J. Histochem. Cytochem.* **1985**, *33*, 77−79.

(36) Xu, F. J.; Yang, X. C.; Li, C. Y.; Yang, W. T. Functionalized Polylactide Film Surfaces *via* Surface-Initiated ATRP. *Macromolecules* **2011**, *44*, 2371−2377.

(37) Liang, B.; He, M. L.; Chan, C.; Chen, Y. C.; Li, X. P.; Li, Y.; Zheng, D. X.; Lin, M. C.; Kung, H. F.; Shuai, X. T.; Peng, Y. The Use of Folate-PEG-Grafted-Hybranched-PEI Nonviral Vector for the Inhibition of Glioma Growth in The Rat. *Biomaterials* **2009**, *30*, 4014−4020.

(38) Hu, Y.; Zhu, Y.; Yang, W. T.; Xu, F. J. New Star-shaped Carriers Composed of β-Cyclodextrin Cores and Disulfide-Linked Poly-(glycidyl methacrylate) Derivative Arms with Plentiful Flanking Secondary Amine and Hydroxyl Groups for Highly Efficient Gene Delivery. *ACS Appl. Mater. Interfaces.* **2013**, *5*, 703−712.

(39) Xiang, S. N.; Tong, H. J.; Shi, Q.; Fernandes, J. C.; Jin, T.; Dai, K. R.; Zhang, X. L. Uptake Mechanisms of Non-viral Gene Delivery. *J. Controlled Release* **2012**, *158*, 371−378.

(40) Kosaka, H.; Ichikawa, T.; Kurozumi, K.; Kambara, H.; Inoue, S.; Maruo, T.; Nakamura, K.; Hamada, H.; Date, I. Therapeutic Effect of Suicide Gene-transferred Mesenchymal Stem Cells in a Rat Model of Glioma. *Cancer Gene Ther.* **2012**, *19*, 572−578.